European Journal of Mechanics B/Fluids 36 (2012) 104–114

Contents lists available at SciVerse ScienceDirect

European Journal of Mechanics B/Fluids

journal homepage: www.elsevier.com/locate/ejmflu

Creeping motion of a porous approximate sphere with an impermeable core in a spherical container

D. Srinivasacharya *, M. Krishna Prasad

Department of Mathematics, National Institute of Technology, Warangal-506 004, A.P., India

ARTICLE INFO

Article history:
Received 14 July 2011
Received in revised form
12 February 2012
Accepted 2 April 2012
Available online 27 April 2012

Keywords:
Porous approximate shell
Spherical container
Brinkman model
Stress jump boundary condition
Wall correction factor

ABSTRACT

The creeping motion of a porous approximate sphere with an impermeable core at the instant it passes the center of a spherical container is discussed. The flow in the spherical container is governed by the Stokes equation. The flow inside the porous approximate sphere is governed by Brinkman's equation. The boundary conditions used at the interface are stress jump condition for tangential stresses, continuity of the normal stresses and velocity components. The drag experienced by the porous approximate spherical particle is obtained. The wall correction factor is calculated. The variations of drag coefficient and wall correction factor are studied with respect to permeability, separation parameters, deformation parameters and stress jump coefficient.

1. Introduction

Several researchers have studied the flow of fluids past porous particles, as they are of great importance in industrial and engineering applications, such as flow through porous beds (fixed or fluidized), sedimentation of fine particulate suspensions, modeling of polymer macromolecule coils in a solvent, catalytic reactions where porous pellets are used, floc settling processes, the flow of oil in oil fields or reservoirs during oil recovery, etc. Porous particles have different geometrical shapes, which differ significantly from spherical. The simplest geometry allowing one to study the effect shape of the permeable particles on their settling velocity and drag resistance is approximate sphere (whose shape deviates slightly from that of a sphere). These applications contain particles in assemblage which may be considered to consist of a number of identical unit cells, each of which contains a particle surrounded by a fluid envelope containing a volume of fluid sufficient to make the fractional void volume in the cell identical to that in the entire assemblage. Furthermore, the outside surface of each cell is assumed to be frictionless. Thus, the entire disturbance due to each particle is confined to the cell of fluid with which it is associated. The unit cell model is the most efficient in the study of concentrated dispersed systems and porous media. This class of problems is important because it provides some information on wall effects. Wall effects for a sphere at the instant it passes the center of the spherical container have been studied by many investigators and these were summarized by Happel and Brenner [1] and Kim and Karrila [2]. On the other hand, only a few studies of wall effects for approximate spheres moving through Newtonian fluids have been attempted. Cunningham [3] and Williams [4], independently, considered the motion of a solid sphere in a spherical container. They presented solutions for the case of an inner solid sphere. Haberman and Sayre [5] studied wall effects for rigid and Newtonian fluid spheres in slow motion with a moving fluid. All the above authors used no-slip condition on the surface of the inner sphere. Ramkissoon and Rahaman [6] studied the motion of solid spherical particle in a spheroidal container using a slip at the surface of the inner particle. They evaluated the expression for drag on the inner sphere and examined the wall effects. They concluded that the wall effects increase as the container becomes more spheroidal. The flow problems of the motion of a porous particles in a container have been modeled by using Stokes' version of the Navier–Stokes equation for the flow inside the container and Darcy's law or Brinkman's equation [7] to describe the flow within the porous particles. The boundary condition for the flow field across a porous-liquid interface has drawn the attention of many researchers. Several types of boundary conditions at the interface of the free fluid and porous region to link the different flow regimes were suggested in literature. One type amongst them is continuity of the velocity, pressure and tangential stresses at the porous-liquid interface. Using this condition, Keh and Chou [8] presented

* Corresponding author. Tel.: +91 870 2462821; fax: +91 870 2459547.
E-mail addresses: dsc@nitw.ac.in, dsrinivasacharya@yahoo.com (D. Srinivasacharya), kpm973.nitw@gmail.com (M. Krishna Prasad).

0997-7546/$ – see front matter © 2012 Elsevier Masson SAS. All rights reserved.
doi:10.1016/j.euromechflu.2012.04.001

Nomenclature

a	radius of solid core
b	radius of porous sphere
c	radius of a spherical container
r_a	radius of an approximate solid sphere
r_b	radius of the porous approximate sphere
k	permeability
k_1	dimensionless parameter ($\sqrt{k}/b$)
U	Uniform velocity
r	radial spherical coordinate
u, v	components of fluid velocity in spherical coordinates
A_n, B_n, C_n, D_n	constants in Eq. (4.1) for the external flow field
E_n, F_n, G_n, H_n	constants in Eq. (4.2) for the flow field inside the porous approximate shell
E^2	Stokesian stream function operator
P_n	Legendre function of the first kind
D	drag force acting on the porous particle
D_∞	drag force acting on the porous particle in an unbounded medium

Greek letters

μ	viscosity of the fluid
σ	stress jump coefficient
ϑ_n	Gegenbauer function
α	Permeability parameter ($b/\sqrt{k}$)
η	dimensionless parameter, defined as (a/b)
λ	dimensionless parameter, defined as (b/c)
θ, ϕ	angular spherical coordinates
ψ	Stokes stream function of the fluid flow
$\beta = \beta_2 = \beta_4$	deformation parameter of the solid core
$\gamma = \gamma_2 = \gamma_4$	deformation parameter of the porous approximate shell

Superscripts

1	fluid inside the spherical container
2	fluid inside the porous approximate shell

an analytical study for the quasi-steady translation and steady rotation of a spherically symmetric composite particle composed of a solid core and a surrounding porous shell located at the center of a spherical cavity filled with an incompressible Newtonian fluid. They evaluated the hydrodynamic drag force and torque exerted by the fluid on the porous particle. They found that the normalized wall-corrected translational and rotational mobilities of the particle decrease monotonically with a decrease in the permeability of its porous shell. The quasi-steady translation and steady rotation of a spherically symmetric porous shell located at the center of a spherical cavity filled with an incompressible Newtonian fluid are investigated analytically by Keh and Lu [9]. They observed that the boundary effects of the cavity wall on the creeping motions of a composite sphere can be quite significant in appropriate situations. The motion of a porous sphere in a spherical container using Brinkman's model in the porous region was studied by Srinivacharya [10]. He calculated the drag force experienced by the porous spherical particle and wall correction factor and studied their variation with permeability. Srinivasacharya [11] has discussed the creeping flow of a viscous fluid past and through a porous approximate sphere neglecting inertia terms, and deduced the result for an oblate spheroid in an unbounded medium. The solution of the problem of symmetrical creeping flow of an incompressible viscous fluid past a swarm of porous approximately spheroidal particles with Kuwabara boundary condition (i.e. the vanishing of vorticity on the boundary) is investigated by Deo and Gupta [12]. They found the dependence of the drag coefficient on permeability for a porous oblate spheroid in an unbounded medium and for a solid oblate spheroid in a cell on the solid volume fraction. The flow problem of an incompressible axisymmetrical quasisteady translation and steady rotation of a porous spheroid in a concentric spheroidal container are studied analytically by Saad [13]. He discussed the dependence of the normalized wall corrected translational and rotational mobilities on permeability for a porous spheroid in an unbounded medium and for a solid spheroid in a cell on the particle volume fraction for various values of the deformation parameter.

Recently, by applying volume average techniques, Ochoa-Tapia and Whitaker [14,15] have investigated the boundary conditions at the porous-liquid interface and have shown that the equations require a discontinuity in the shearing stress but continuity in velocity components and normal stress. They derived the stress jump boundary condition

$$\epsilon^{-1}\frac{\partial u^p}{\partial y} - \frac{\partial u^l}{\partial y} = \frac{\sigma}{\sqrt{k}}\,u^p$$

where u^p, u^l are tangential velocity components in porous region and liquid region respectively. ϵ is the porosity, k is the permeability of the homogeneous portion of the porous region and σ is the stress jump coefficient. If $\sigma \neq 0$, there is a discontinuity in the shear stress at the porous-liquid interface. This jump condition is constructed to join Darcy's law with the Brinkman correction to Stokes equations. Experimentally it has been verified that the jump coefficient σ varies in the range -1 to 1 [14–17]. Kuznetsov [16,17] used this stress jump boundary condition at the interface between a porous medium and a clear fluid to discuss flow in channels partially filled with a porous medium. Bhattacharyya and Raja Sekhar [18,19] have used stress jump boundary condition while discussing the Stokes flow of a viscous fluid inside a sphere with internal singularities, enclosed by a porous spherical shell and in discussing arbitrary viscous flow past a porous sphere with an impermeable core. They concluded that the fluid velocity at a porous-liquid interface varies with the stress jump coefficient and it plays an important role in describing the flow field associated with porous medium. Srivastava and Srivastava [20] studied the Stokes flow through a porous sphere with a solid core using the stress jump condition at the fluid-porous interface and matched Stokes' and Oseen's solutions far away from the sphere. They concluded that drag on a porous sphere decreases with increasing permeability of the medium. Yadav et al. [21] studied slow viscous flow through a swarm of porous spherical particles using the stress jump condition at the fluid-porous interface and four known boundary conditions (Happel's, Kuwabara's, Kvashnin's and Cunningham's (Mehta-Morse's condition)) on the hypothetical surface are considered and compared. They concluded that the jump condition for tangential stresses at the interface between porous medium and clear liquid gives a good possibility to take into account the influence of slipping on the hydrodynamic permeability of membranes having globular structure in comparison.

In this paper, we considered the creeping motion of a porous approximate sphere with an impermeable core in a spherical container. The flow examined is axially symmetric in nature. The flow in the spherical container is governed by the Stokes equations. The flow within the porous region is governed by Brinkman's equation. As boundary conditions, continuity of the velocity, pressure and the slip condition at the interface proposed by Octoa-Tapia are employed. The stream function and the pressure for both the flows inside porous particle and within the spherical container are calculated. The drag experienced by the porous

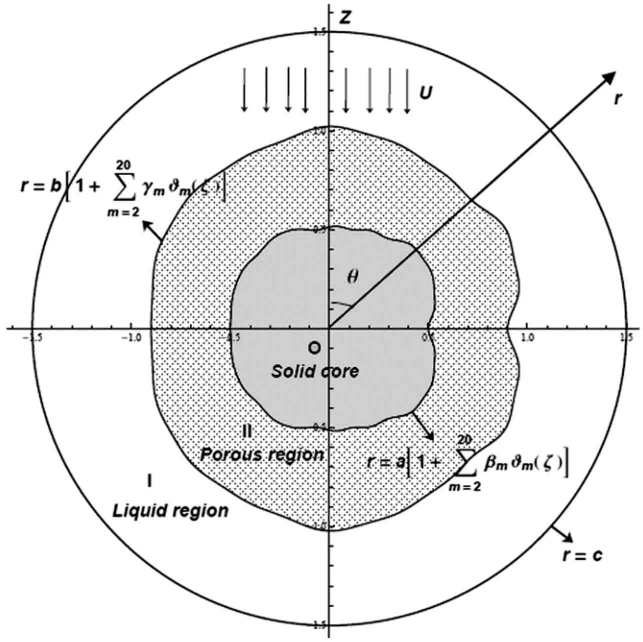

Fig. 1. The physical situation and the coordinate system.

approximate sphere is evaluated numerically for different values of permeability, stress jump coefficient, separation parameters and deformation parameters. The wall correction factor is calculated and its variation is studied numerically.

2. Formulation of the problem

Consider a porous approximate spherical particle of radius $r = b[1 + \sum_{m=2}^{\infty} \gamma_m \vartheta_m(\zeta)] \equiv r_b$ [1] with impermeable core of radius $r = a[1 + \sum_{m=2}^{\infty} \beta_m \vartheta_m(\zeta)] \equiv r_a (r_a < r_b)$ passing the center of a spherical vessel of radius $c (r_b < c)$ containing an incompressible Newtonian viscous fluid. Here β_m and γ_m are small, $\vartheta_n(\zeta)$, $(\zeta = \cos\theta)$ is the Gegenbauer function of the first kind of order n and degree $-1/2$. If all the β_m and γ_m are zero, the approximate spherical shell reduces to spherical shell of external and internal radii b and a respectively. The liquid region $(c \leq r \leq r_b)$ and the porous region $(r_b \leq r \leq r_a)$ are denoted by regions I and II respectively. This is equivalent to the inner particle at rest while the outer spherical container moves with a constant velocity **U** in the negative Z-direction. We assume that the flow within the spherical container is governed by Stokes' equation and flow inside the porous approximate spherical shell is governed by Brinkman's model.

The equations of motion for the region within the spherical container (region I) are

$$\nabla \cdot \vec{q}^{(1)} = 0, \tag{2.1a}$$

$$\nabla p^{(1)} + \mu \nabla \times \nabla \times \vec{q}^{(1)} = 0 \tag{2.1b}$$

where $\vec{q}^{(1)}$ is the volumetric average of the velocity, μ is the coefficient of viscosity and $p^{(1)}$ is the average of the pressure.

For the region inside the porous approximate spherical shell (region II), the equations of motion are

$$\nabla \cdot \vec{q}^{(2)} = 0, \tag{2.2a}$$

$$\nabla p^{(2)} + \frac{\mu}{k} \vec{q}^{(2)} + \mu \nabla \times \nabla \times \vec{q}^{(2)} = 0 \tag{2.2b}$$

where $\vec{q}^{(2)}$ is the volumetric average of the velocity, μ is the coefficient of viscosity, $p^{(2)}$ is the average of the pressure and k is the permeability of the porous medium.

Let (r, θ, ϕ) denote a spherical polar co-ordinate system with the origin at the center of the sphere of radius a. Since the flow of the fluid is in the meridian plane and the flow is axially symmetric, all the physical quantities are independent of ϕ. Hence, we assume that the velocity vectors $\vec{q}^{(1)}$ and $\vec{q}^{(2)}$ in the form

$$\vec{q}^{(i)} = u^{(i)}(r, \theta)\vec{e}_r + v^{(i)}(r, \theta)\vec{e}_\theta, \quad i = 1, 2 \tag{2.3}$$

where $(\vec{e}_r, \vec{e}_\theta, \vec{e}_\phi)$ unit base vectors (see Fig. 1).

In view of the incompressibility condition $\nabla \cdot \vec{q}^{(i)} = 0, i = 1, 2$, we introduce the stream function $\psi^{(i)}(r, \theta), i = 1, 2$, through

$$u^{(i)} = -\frac{1}{r^2 \sin\theta} \frac{\partial \psi^{(i)}}{\partial \theta}; \qquad v^{(i)} = \frac{1}{r \sin\theta} \frac{\partial \psi^{(i)}}{\partial r}, \quad i = 1, 2. \tag{2.4}$$

Eliminating pressure from (2.1) and (2.2), and substituting (2.4) in the resulting equations, we get the following dimensionless equations for $\psi^{(i)}, i = 1, 2$:

$$E^4 \psi^{(1)} = 0, \tag{2.5}$$

$$E^2(E^2 - \alpha^2)\psi^{(2)} = 0 \tag{2.6}$$

where $\alpha^2 = b^2/k$ and $E^2 = \frac{\partial^2}{\partial r^2} + \frac{(1-\zeta^2)}{r^2} \frac{\partial^2}{\partial \zeta^2}$ is the Stokesian stream function operator.

3. Boundary conditions

To determine the flow velocity and pressure outside and inside the porous approximate shell, we use the following boundary conditions:

(i) The normal velocity component is continuous at the porous boundary, i.e.,

$$u^{(1)}(r, \theta) = u^{(2)}(r, \theta) \quad \text{on } r = r_b. \tag{3.1}$$

(ii) The tangential velocity component is continuous at the porous boundary, i.e.,

$$v^{(1)}(r, \theta) = v^{(2)}(r, \theta) \quad \text{on } r = r_b. \tag{3.2}$$

(iii) Continuity of the pressure distributions at the porous boundary, i.e.,

$$p^{(1)}(r, \theta) = p^{(2)}(r, \theta) \quad \text{on } r = r_b. \tag{3.3}$$

(iv) Ochoa-Tapia's stress jump boundary condition for tangential stress, i.e.,

$$\frac{\partial v^{(2)}}{\partial r} - \frac{\partial v^{(1)}}{\partial r} = \frac{\sigma}{\sqrt{k}} v^{(2)} \quad \text{on } r = r_b \tag{3.4}$$

where σ is the stress jump coefficient.

(v) On the impermeable core, i.e.,

$$u^{(2)}(r, \theta) = 0 \quad \text{and} \quad v^{(2)}(r, \theta) = 0 \quad \text{on } r = r_a. \tag{3.5}$$

(vi) On the spherical container, the condition of impenetrability leads to

$$u^{(1)}(r, \theta) = -U\cos\theta \quad \text{and} \quad v^{(1)}(r, \theta) = U\sin\theta \quad \text{on } r = c \tag{3.6}$$

and the condition that velocity and pressure must have no singularities anywhere in the flow field.

4. Solution of the problem

For the region I, the solution of (2.5) which is regular at infinity is

$$\psi^{(1)} = \sum_{n=2}^{\infty} \left[A_n r^n + B_n r^{-n+1} + C_n r^{n+2} + D_n r^{-n+3}\right] \times \vartheta_n(\zeta). \tag{4.1}$$

For the region II, the solution of (2.6) is given by

$$\psi^{(2)} = \sum_{n=2}^{\infty} \left[E_n\, r^n + F_n\, r^{-n+1} + G_n \sqrt{r}\, K_{n-1/2}(\alpha\, r) + H_n \sqrt{r}\, I_{n-1/2}(\alpha\, r)\right] \vartheta_n(\zeta) \tag{4.2}$$

where $I_{n-1/2}(\alpha r)$ and $K_{n-1/2}(\alpha r)$ denotes the modified Bessel functions of the first kind and second kind of order $n - 1/2$ respectively.

Using the Eqs. (4.1) and (4.2), the expressions for the pressure in the both flow regions are

$$p^{(1)} = -\sum_{n=2}^{\infty} \left[C_n \left(\frac{4\,n+2}{n-1}\right) r^{n-1} - D_n \left(\frac{6-4\,n}{n}\right) r^{-n}\right] \times P_{n-1}(\zeta), \tag{4.3}$$

$$p^{(2)} = \alpha^2 \sum_{n=2}^{\infty} \left(E_n \frac{r^{n-1}}{n-1} - F_n \frac{r^{-n}}{n}\right) P_{n-1}(\zeta) \tag{4.4}$$

where $P_n(\zeta)$ is Legendre function of the first kind.

5. Determination of arbitrary constants

The boundary conditions from Eqs. (3.1) to (3.6) in terms of the stream function in dimensionless form are

$$\left.\begin{aligned} &\psi^{(1)}(r,\theta) = \psi^{(2)}(r,\theta), \quad \psi_r^{(1)}(r,\theta) = \psi_r^{(2)}(r,\theta),\\ &\psi_{rr}^{(2)} - \psi_{rr}^{(1)} = \alpha\,\sigma\,\psi_r^{(2)}, \quad p^{(1)}(r,\theta) = p^{(2)}(r,\theta), \end{aligned}\right\}$$
$$\text{on } r = 1 + \gamma_m\,\vartheta_m(\zeta) \tag{5.1}$$

$$\psi^{(2)}(r,\theta) = 0, \qquad \psi_r^{(2)}(r,\theta) = 0,$$
$$\text{on } r = \eta\,[1 + \beta_m\,\vartheta_m(\zeta)] \tag{5.2}$$

$$\psi^{(1)}(r,\theta) = \frac{1}{2} r^2 \sin^2\theta, \qquad \psi_r^{(1)}(r,\theta) = r\sin^2\theta$$
$$\text{on } r = 1/\lambda \tag{5.3}$$

where $\eta = a/b$ and $\lambda = b/c$.

We first develop the solution corresponding to the boundaries $r = 1 + \gamma_m\,\vartheta_m(\zeta)$, $r = \eta[1 + \beta_m\,\vartheta_m(\zeta)]$ and $r = 1/\lambda$. Assume that the coefficients γ_m and β_m are sufficiently small so that squares and higher powers of γ_m and β_m can be neglected [1] i.e., $r^y \approx 1 + y\gamma_m\vartheta_m(\zeta)$ and $r^y \approx \eta^y[1 + y\beta_m\vartheta_m(\zeta)]$ where y is positive or negative. Comparison of the Eqs. (4.1) and (4.2) with those obtained in case of flow of an incompressible viscous fluid past a porous spherical shell, indicates that the terms involving A_n, B_n, C_n, D_n, E_n, F_n, G_n and H_n for $n > 2$ are the extra terms here which are not present in the case of spherical shell. The body that we are considering is an approximate spherical shell and the flow generated is not expected to be very different from the one generated by flow past a porous spherical shell [22]. Also the coefficients A_n, B_n, C_n, D_n, E_n, F_n, G_n, H_n for $n > 2$ are of order γ_m and the coefficients E_n, F_n, G_n and H_n for $n > 2$ are of order β_m. Therefore, while implementing the boundary conditions, we ignore the departure from the spherical form and set in (5.1) $r = 1$ in the terms involving $A_n, B_n, C_n, D_n, E_n, F_n, G_n, H_n$ for $n > 2$ and in (5.2) $r = \eta$ in the terms involving E_n, F_n, G_n and H_n for $n > 2$.

Applying the boundary conditions (5.1)–(5.3) to the first order in γ_m and β_m, we have evaluated all the coefficients appearing in the stream functions (4.1) and (4.2) for the case of porous spherical shell and for the case of porous approximate spherical shell, where only drag is given. These coefficients are mentioned in the Appendix. Thus the stream functions for regions I and II are given by

$$\begin{aligned}\psi^{(1)} = {} & \left[A_2\, r^2 + B_2\, r^{-1} + C_2\, r^4 + D_2\, r\right] \vartheta_2(\zeta) \\ & + \sum_{m=2}^{\infty}\Big\{\left[A_{m-2}\, r^{m-3} + B_{m-2}\, r^{-m+3} + C_{m-2}\, r^m + D_m\, r^{-m+5}\right] \vartheta_{m-2}(\zeta) + \left[A_m\, r^m + B_m\, r^{-m+1} \right.\\ & \left. + C_m\, r^{m+2} + D_m\, r^{-m+3}\right] \vartheta_m(\zeta) + \left[A_{m+2}\, r^{m+2} + B_{m+2}\, r^{-m-1} + C_{m+2}\, r^{m+4} + D_{m+2}\, r^{-m+1}\right] \\ & \times \vartheta_{m+2}(\zeta)\Big\},\end{aligned} \tag{5.4}$$

$$\begin{aligned}\psi^{(2)} = {} & \left[E_2\, r^2 + F_2\, r^{-1} + G_2 \sqrt{r}\, K_{3/2}(\alpha\, r) + H_2 \sqrt{r}\, I_{3/2}(\alpha\, r)\right] \vartheta_2(\zeta) + \sum_{m=2}^{\infty}\Big\{\left[E_{m-2}\, r^{m-2} \right.\\ & \left. + F_{m-2}\, r^{-m+3} + G_{m-2} \sqrt{r}\, K_{m-5/2}(\alpha\, r) + H_{m-2} \sqrt{r}\, I_{m-5/2}(\alpha\, r)\right] \vartheta_{m-2}(\zeta) \\ & + \left[E_m\, r^m + F_m\, r^{-m+1} + G_m \sqrt{r}\, K_{m-1/2}(\alpha\, r) + H_m \sqrt{r}\, I_{m-1/2}(\alpha\, r)\right] \vartheta_m(\zeta) \\ & + \left[E_{m+2}\, r^{m+2} + F_{m+2}\, r^{-m-1} + G_{m+2} \sqrt{r}\, K_{m+3/2}(\alpha\, r) + H_{m+2} \sqrt{r}\, I_{m+3/2}(\alpha\, r)\right] \vartheta_{m+2}(\zeta)\Big\}.\end{aligned} \tag{5.5}$$

6. Drag on the body and wall effects

The drag force acting on the porous approximate spherical shell is given by

$$\mathcal{F} = \mu\,\pi \int_0^{\pi} \varpi^3 \frac{\partial}{\partial r}\left(\frac{E^2\,\psi^{(1)}}{\varpi^2}\right) r\, d\theta \tag{6.1}$$

where $\varpi = r\sin\theta$.
Using Eq. (4.1) and on carrying out the integration it is found to be

$$\mathcal{D} = 4\,\mu\,\pi\, U\, b\left(D_2 + \frac{1}{5}\,\mathcal{D}_2' + \frac{2}{35}\,\mathcal{D}_2''\right) \tag{6.2}$$

where D_2, $\mathcal{D}_2'$, $\mathcal{D}_2''$ are given in the Appendix.

As $c \to \infty$ (or $\lambda \to 0$), we get the drag on a porous approximate sphere with impermeable core in case of streaming in an unbounded medium,

$$\mathcal{D}_\infty = 4\,\pi\,\mu\, U\, b\left[\Delta_1 + \frac{1}{5}\,\Delta_2 + \frac{2}{35}\,\Delta_3\right] \tag{6.3}$$

where Δ_1, Δ_2, Δ_3 are given in the Appendix.

The wall correction factor W_c is defined as the ratio of the actual drag experienced by the particle in the enclosure and the drag on a particle in an infinite expanse of fluid. With the aid of Eqs. (6.2) and (6.3) this becomes

$$\mathcal{W}_c = \frac{\mathcal{D}}{\mathcal{D}_\infty}. \tag{6.4}$$

Note that $\mathcal{W}_c = 1$ as $\lambda \to 0$ and $\mathcal{W}_c \geq 1$ as $0 < \lambda \leq 1$.

6.1. Special cases

6.1.1. Porous sphere with an impermeable core in a spherical container

If $\beta_m = 0$ and $\gamma_m = 0$ for $m > 2$, the approximate spheres reduces to spheres and the drag experienced by the porous sphere with an impermeable core is

$$\mathcal{D} = 4\,\pi\,\mu\, U\, b\, D_2. \tag{6.5}$$

As $c \to \infty$ ($\lambda \to 0$), $\beta_m = 0$ and $\gamma_m = 0$ for $m > 2$, we get the drag on a porous sphere with impermeable core in the case of streaming in an unbounded medium,

$$\mathcal{D}_\infty = 4\,\pi\,\mu\, U\, b\,\Delta_1. \tag{6.6}$$

6.1.2. Porous sphere in a spherical container

As $a \to 0$ (or $\eta \to 0$), we get the drag on a porous sphere in a spherical container,

$$\mathcal{D} = 24\pi\,\mu\,U\,b\,\alpha\left[\alpha\,\left(15\,\lambda^5\,(\alpha-2\,\sigma)+\alpha^2\,(\alpha+\sigma)\right.\right.$$
$$\times\,\left.(\lambda^5-1)\right)\,\cosh\alpha-\left(15\,\lambda^5\,(\alpha-2\,\sigma)+\alpha^3\,(6\,\lambda^5-1)\right.$$
$$\left.\left.+\alpha^2\,\sigma\,(\alpha^2\,(\lambda^5-1)-(9\,\lambda^5+1))\right)\,\sinh\alpha\right]/L_1 \quad (6.7)$$

where

$$L_1 = \alpha\,\left(-270\,\lambda^5+\alpha^3\,(\alpha+\sigma)\,(\lambda-1)^4\,(4\,\lambda^2+7\,\lambda+4)\right.$$
$$+6\,\alpha^2\,(10\,\lambda^6-21\,\lambda^5+10\,\lambda^3+1)$$
$$\left.-6\,\alpha\,\sigma\,(20\,\lambda^6-9\,\lambda^5-10\,\lambda^3-1)\right)\,\cosh\alpha$$
$$-\left(-270\,\lambda^5+3\,\alpha^4\,(\lambda-1)^3\,\lambda\,\,(8\,\lambda^2+9\,\lambda+3)\right.$$
$$+6\,\alpha^2\,(10\,\lambda^6-36\,\lambda^5+10\,\lambda^3+1)$$
$$-6\,\alpha\,\sigma\,(20\,\lambda^6-9\,\lambda^5-10\,\lambda^3-1)$$
$$-3\,\alpha^3\,\sigma\,(12\,\lambda^6-3\,\lambda^5-10\,\lambda^3+3\,\lambda-2)$$
$$\left.+\alpha^5\,(\lambda-1)^4\,\sigma\,(4\,\lambda^2+7\,\lambda+4)\right)\,\sinh\alpha.$$

If $\sigma = 0$, i.e., the continuity of the shear stress, the drag is given by

$$\mathcal{D} = 24\pi\,\mu\,U\,b\,\alpha^2\,\left[\alpha\,\left(15\,\lambda^5+\alpha^2(\lambda^5-1)\right)\cosh\alpha\right.$$
$$\left.-\left(15\,\lambda^5+\alpha^2(6\,\lambda^5-1)\right)\sinh\alpha\right]/L_2 \quad (6.8)$$

where

$$L_2 = \alpha\,\left(-270\,\lambda^5+\alpha^4(\lambda-1)^4(4\,\lambda^2+7\,\lambda+4)\right.$$
$$\left.+6\,\alpha^2(10\,\lambda^6-21\,\lambda^5+10\,\lambda^3+1)\right)\cosh\alpha$$
$$-\left(-270\,\lambda^5+3\,\alpha^4(\lambda-1)^3\lambda(8\,\lambda^2+9\,\lambda+3)\right.$$
$$\left.+6\,\alpha^2\,(10\,\lambda^6-36\,\lambda^5+10\,\lambda^3+1)\right)\sinh\alpha$$

which agrees with the drag on the porous sphere case derived by Srinivacharya [10].

As $a \to 0$ and $c \to \infty$ ($\eta \to 0$ and $\lambda \to 0$), we get the drag on a porous sphere in the case of streaming in an unbounded medium,

$$\mathcal{D}_\infty = \frac{12\,\mu\,\pi\,U\,b\,\alpha^2\,\left(-\alpha\,(\alpha+\sigma)\,\cosh\alpha+(\alpha+\sigma\,(1+\alpha^2))\,\sinh\alpha\right)}{\alpha\,(3+2\,\alpha^2)(\alpha+\sigma)\,\cosh\alpha-(3\,\alpha+(3\,(1+\alpha^2)+2\,\alpha^4)\,\sigma)\,\sinh\alpha}. \quad (6.9)$$

If $\sigma = 0$, i.e., the continuity of the shear stress, the drag is given by

$$\mathcal{D}_\infty = \frac{12\,\mu\,\pi\,U\,b\,\alpha^2\,\left(-\alpha\,\cosh\alpha+\sinh\alpha\right)}{\alpha\,(3+2\,\alpha^2)\,\cosh\alpha-3\,\sinh\alpha} \quad (6.10)$$

which agrees with the porous sphere case derived by Brinkman [7], and Neale et al. [23].

6.1.3. Solid sphere in a spherical container

As $\eta \to 1$ (or $k \to 0$), we get the drag on a solid sphere in a spherical container

$$\mathcal{D} = 24\pi\,\mu\,U\,b\,\frac{\left(\lambda^4+\lambda^3+\lambda^2+\lambda+1\right)}{\left(4\,\lambda^2+7\,\lambda+4\right)(\lambda-1)^3} \quad (6.11)$$

which agrees with the solid sphere in a spherical container derived by Ramkissoon and Rahaman [6].

If $\lambda \to 0$,

$$\mathcal{D}_\infty = -6\,\mu\,\pi\,U\,b \quad (6.12)$$

which is a well known result (Stokes' law) for flow past a solid sphere in an unbounded medium.

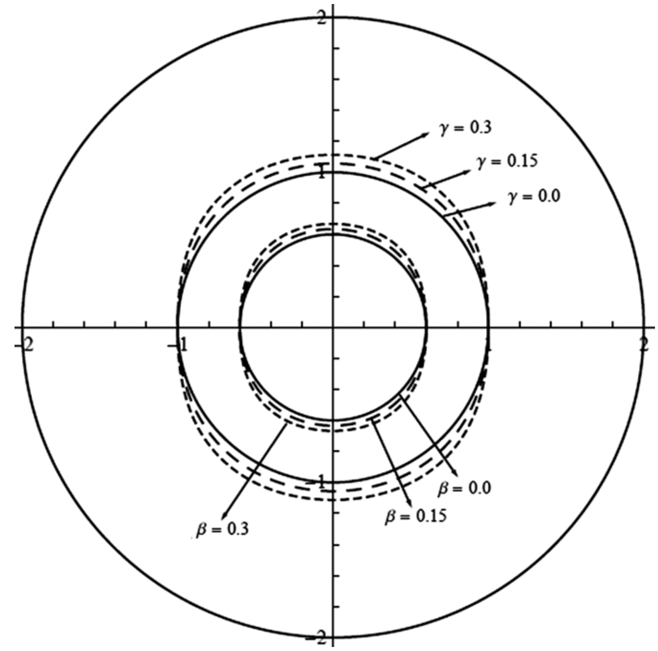

Fig. 2. The shape of the particle with varying deformation parameters $\gamma = \gamma_2 = \gamma_4, \beta = \beta_2 = \beta_4$ and the separation parameters $\eta = 0.6$ and $\lambda = 0.5$.

7. Results and discussion

The drag coefficient $\mathcal{D}_N = \mathcal{D}/(4\pi\mu Ub)$ is numerically computed for various values of $k_1(= 1/\alpha = \sqrt{k}/b)$, $\gamma = \gamma_2 = \gamma_4$, $\beta = \beta_2 = \beta_4, \sigma, \lambda$ and η and its variation is presented in Figs. 3–7. The parameter k_1 represents the permeability parameter. The parameters γ and β characterize the deformations of porous shell and solid core respectively. The parameters $\eta = a/b$ and $\lambda = b/c$ are the separation parameters which represent the extent of closeness between the solid core and particle, and particle and the cavity wall respectively. The changes of shape from porous spherical particle with spherical solid core to porous approximate spherical particle with approximate spherical core are shown Fig. 2.

The variation of $\mathcal{D}_N$ with permeability k_1, λ and η for various values of γ is shown in Fig. 3 when $\beta = 0.1$ and $\sigma = 0$ (the continuity of the tangential stresses). In particular, Fig. 3(a) presents the effects of λ and γ on drag coefficient. It is observed that increasing permeability parameter k_1 decreases the drag coefficient. When there is no deformation of the porous shell, i.e. $\gamma = 0$, the drag is increasing for increasing values of the separation parameter λ. Also, increasing the deformation parameter γ increases the drag coefficient for all values of the permeability. But this behavior of drag coefficient with γ changes at some value of permeability k_1, beyond which the drag coefficient decreases for $\lambda > 0.5$. This particular value of the permeability is decreasing as the parameter λ tends to 1. Further, the drag coefficient decreases significantly after some particular values of k_1 as γ increases and $\lambda \to 1$. This is because of the increase in the pressure in the spherical container when the thickness of the cavity region decreases (i.e. $\lambda \to 1$). In this case the porous particle with solid core occupies whole spherical container except at the deformations of the particle.

Fig. 3(b) shows the effect of η and γ on the drag coefficient. It is clear from this figure that increasing η, i.e. decreasing the thickness of the porous region increases the drag coefficient when there is no deformation of the porous shell ($\gamma = 0$). The drag coefficient is increasing for increasing values of the deformation of the porous shell γ. But as η increases and also the deformation of the porous shell increases, the behavior of the drag coefficient changes at some value of permeability k_1, beyond which the drag coefficient

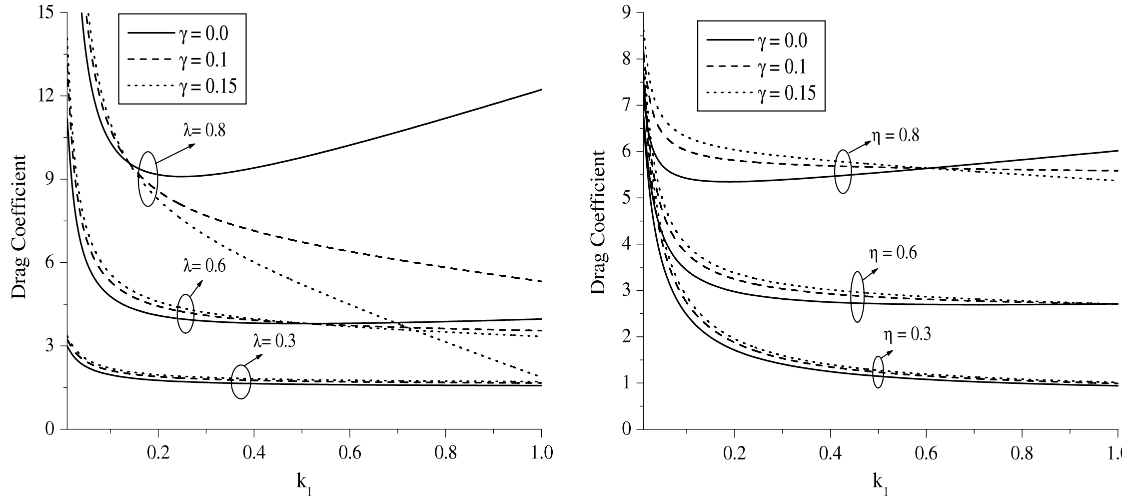

(a) Variation of $\mathcal{D}_N$ with λ and γ for $\eta = 0.6$. (b) Variation of $\mathcal{D}_N$ with η and γ for $\lambda = 0.5$.

Fig. 3. Variation of drag coefficient $\mathcal{D}_N$ with k_1, λ, η and γ for $\sigma = 0$, $\beta = 0.1$.

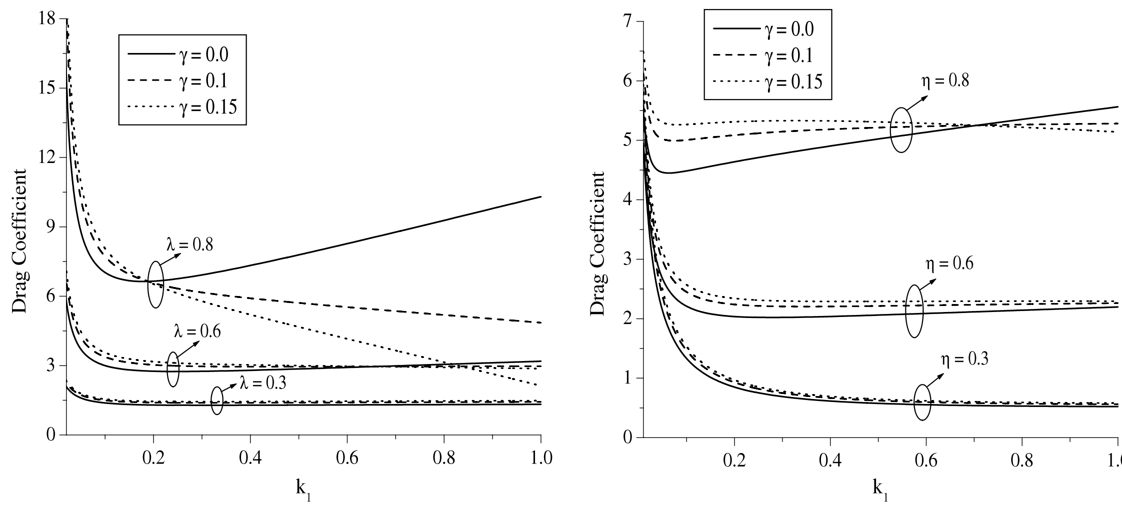

(a) Variation of $\mathcal{D}_N$ with λ and γ for $\eta = 0.6$. (b) Variation of $\mathcal{D}_N$ with η and γ for $\lambda = 0.5$.

Fig. 4. Variation of drag coefficient $\mathcal{D}_N$ with k_1, λ, η and γ for $\sigma = 0.5$, $\beta = 0.1$.

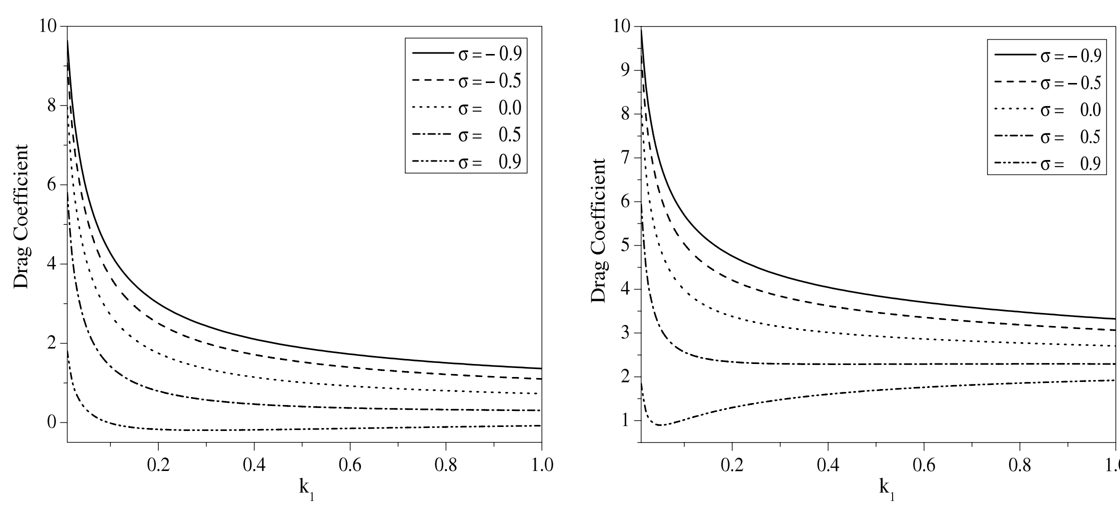

(a) Variation of $\mathcal{D}_N$ with γ for $\eta = 0.2$. (b) Variation of $\mathcal{D}_N$ with γ for $\eta = 0.6$.

Fig. 5. Variation of drag coefficient $\mathcal{D}_N$ with k_1 and σ for $\gamma = 0.15$, $\beta = 0.1$, $\lambda = 0.5$.

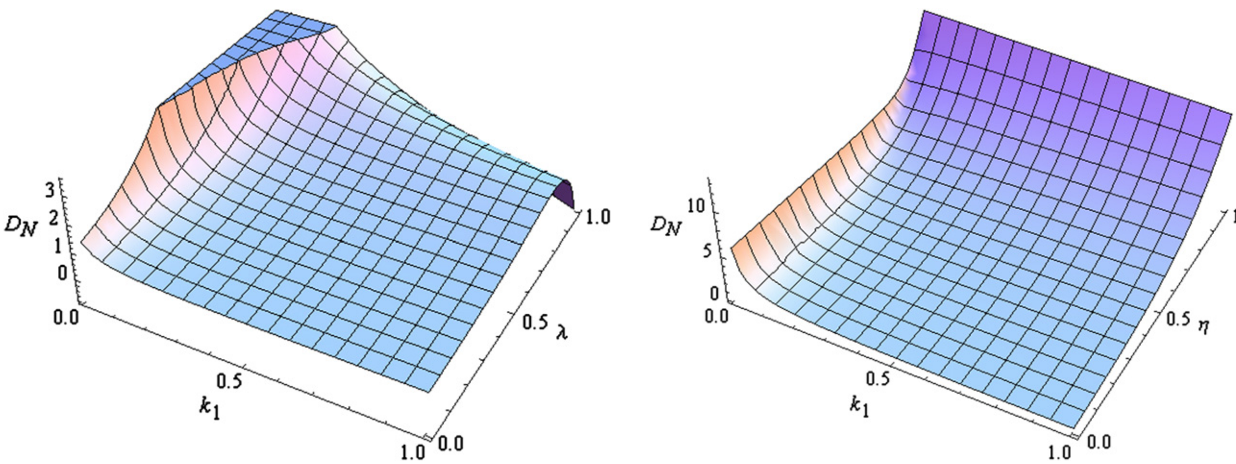

(a) Variation of $\mathcal{D}_N$ with λ and k_1 for $\eta = 0.4$.

(b) Variation of $\mathcal{D}_N$ with η and k_1 for $\lambda = 0.5$.

Fig. 6. Variation of drag coefficient $\mathcal{D}_N$ with λ, η and k_1 for $\sigma = 0.5$, $\beta = 0.1$, $\gamma = 0.15$.

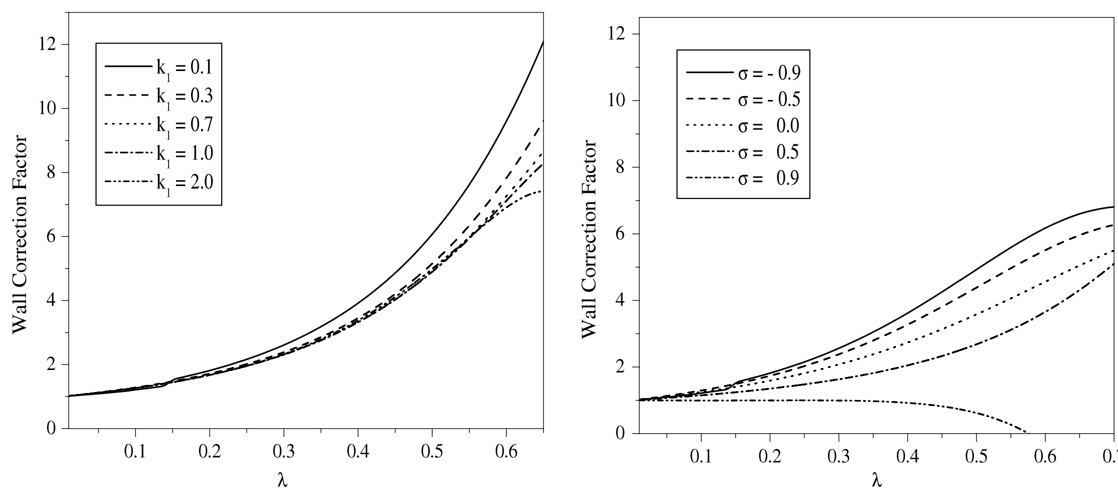

(a) Variation of $\mathcal{W}_c$ with k_1 for $\sigma = 0$.

(b) Variation of $\mathcal{W}_c$ with σ for $k_1 = 0.4$.

Fig. 7. Variation of wall correction factor $\mathcal{W}_c$ with separation parameter λ for $\eta = 0.3$, $\beta = 0.1$, $\gamma = 0.15$.

decreases. This particular value of the permeability is decreasing as the parameter $\eta \to 1$. As η tends to 1, i.e. the distance between the solid core and the porous particle decreases, the porous particle with solid core in the spherical container becomes a solid particle except at the deformations of the solid core and porous particle. Hence the particular value of the permeability, at which the drag changes its behavior, decreases.

Fig. 4 depicts the variation of drag coefficient $\mathcal{D}_N$ with permeability k_1 for various values of γ, λ, and η when $\beta = 0.1$ and $\sigma = 0.5$ (i.e. when there is a jump in the stress). The drag coefficient is increasing for increasing values of γ and then decreasing beyond some value of permeability k_1 for increasing values of λ (Fig. 4(a)) and η (Fig. 4(b)). The particular value of k_1, at which drag changes its behavior for the case of $\sigma = 0.5$ is more than the case of $\sigma = 0$. Also the drag coefficient decreases when there is a jump in stress.

The variation of drag coefficient with k_1 and σ for $\gamma = 0.15$, $\beta = 0.1$, $\lambda = 0.5$ is plotted in Fig. 5. The values of σ are taken in the range -1 to 1 as proposed by Ochoa-Tapia and Whitaker [14,15]. The validity of these values of σ along with the combination of other parameters and permeability is examined for the present problem so that the drag experienced by the porous approximate sphere give a physical significance. The effects of the stress jump coefficient σ on the drag coefficient are presented in Fig. 5(a) for $\eta = 0.2$ i.e., when the thickness of the porous region is large. It is observed from this figure that the drag coefficient is decreasing for increasing values of the stress jump coefficient. For positive values of stress jump coefficient σ, there is a reversal in the behavior of drag at a particular value of permeability. Beyond the value of this particular permeability, the value of drag becomes negative which is not physically possible. Therefore, the positive values of σ can not be considered beyond that particular permeability. If negative values of σ are considered in the stress jump condition (3.4) the shear stress of external free flow region becomes more than that of the internal (porous) flow region which generates a significant drag force on the porous surface. Even though the shear stress of the external region is low for positive values of σ, a significant drag force is generated on the surface for particular range of permeability. In Fig. 5(b) for $\eta = 0.6$, it is noticed that the drag coefficient is increasing for increasing values of η and is always positive for all values of the stress jump coefficient.

The influence of separation parameters λ and η on the drag coefficient with permeability parameter k_1 is depicted in Fig. 6. The variation of drag coefficient versus λ and permeability k_1 is shown in Fig. 6(a). It is seen that increasing λ increases $\mathcal{D}_N$. Increasing permeability k_1 decreases the drag coefficient. The variation of drag coefficient versus η and permeability k_1 is shown in Fig. 6(b). It is observed that $\mathcal{D}_N$ is increasing for increasing values of η.

The variation of wall correction factor $\mathcal{W}_c$ against the separation parameter λ with continuity of tangential stress ($\sigma = 0$) for various values of permeability k_1 is shown in Fig. 7(a). It can be observed from the figure that increasing λ increases the wall correction. The wall correction factor is decreasing for increasing values of the permeability parameter k_1. For $k_1 > 1$, the particle mobility varies slowly with the separation parameter λ, compared with the case of lower permeability. The effect of the stress jump coefficient σ and separation parameter λ on wall correction factor $\mathcal{W}_c$ has been plotted in Fig. 7(b). It is noticed that the wall corrector factor is increasing for increasing values of λ. The magnitude of the correction factor decreases as the jump coefficient increases. The correction factor depends on the stress jump coefficient and separation parameter λ. So, a jump in the tangential stress at the boundary of the porous-liquid interface cannot be ignored.

8. Conclusions

In this paper, the creeping motion of a porous approximate spherical shell enclosed with an approximate spherical solid core in a concentric spherical cavity filled with an incompressible Newtonian fluid have been investigated. An analytical solution is obtained by considering Brinkman's model in the porous region and Stokes' equation in the liquid region. At the porous-liquid interface, the stress jump boundary condition for tangential stress, continuity of normal stress and continuity of velocities components have been used. The hydrodynamic drag force experienced by the porous approximate spherical shell is obtained in the closed form (6.2) in terms of the parameters $\eta(=a/b)$, $\lambda(=b/c)$, $\alpha(=b/\sqrt{k})$, and σ. The drag decreases with the increasing permeability along with increasing the stress jump coefficient σ. It is found that there is a significant effect of the stress jump coefficient σ on the hydrodynamic drag. The wall correction factor for porous approximate shell in the presence of a cavity wall is obtained. It is seen that the effect of a stress jump coefficient in a bounded medium is significant. Therefore, one has to take the stress jump in the tangential stress components into consideration, which has a significant impact on the physical problem.

Acknowledgments

The authors are thankful to the reviewers for their valuable suggestions and comments.

Appendix

Applying the boundary conditions (5.1) and (5.2) to the first order in β_m and γ_m and (5.3), we obtain the following system of algebraic equations

$$\begin{aligned}&\big[A_2+B_2+C_2+D_2-E_2-F_2\\&\quad-K_{3/2}(\alpha)\,G_2-I_{3/2}(\alpha)\,H_2\big]\vartheta_2(\zeta)\\&\quad+[2\,A_2-B_2+4\,C_2+D_2-2\,E_2+F_2]\\&\quad\times\gamma_m\,\vartheta_m(\zeta)\,\vartheta_2(\zeta)+\sum_{n=3}^{\infty}\big[A_n+B_n+C_n+D_n-E_n\\&\quad-F_n-K_{n-1/2}(\alpha)\,G_n-I_{n-1/2}(\alpha)\,H_n\big]\,\vartheta_n(\zeta)=0\end{aligned}\tag{A.1}$$

$$\begin{aligned}&\big[2\,A_2-B_2+4\,C_2+D_2-2\,E_2+F_2+\big(K_{3/2}(\alpha)\\&\quad+\alpha\,K_{1/2}(\alpha)\big)\,G_2+\big(I_{3/2}(\alpha)-\alpha\,I_{1/2}(\alpha)\big)\,H_2\big]\,\vartheta_2(\zeta)\\&\quad+\big[2\,A_2+2\,B_2+12\,C_2-2\,E_2-2\,F_2-K_{3/2}(\alpha)\,G_2\\&\quad-I_{3/2}(\alpha)\,H_2\big]\,\gamma_m\,\vartheta_m(\zeta)\,\vartheta_2(\zeta)\\&\quad+\sum_{n=3}^{\infty}\big[n\,A_n-(n-1)\,B_n+(n+2)\,C_n-(n-3)\,D_n\\&\quad-n\,E_n+(n-1)\,F_n+\big((n-1)\,K_{n-1/2}(\alpha)\\&\quad+\alpha\,K_{n-3/2}(\alpha)\big)\,G_n+\big((n-1)\,I_{n-1/2}(\alpha)-\alpha\,I_{n-3/2}(\alpha)\big)\\&\quad\times H_n\big]\,\vartheta_n(\zeta)=0\end{aligned}\tag{A.2}$$

$$\begin{aligned}&[-2\,A_2-2\,B_2-12\,C_2+2\,(1-\alpha\,\sigma)\,E_2+(2+\alpha\,\sigma)\,F_2\\&\quad+\big((\alpha^2+\alpha\,\sigma+2)\,K_{3/2}(\alpha)+\alpha^2\,\sigma\,K_{1/2}(\alpha)\big)\,G_2\\&\quad+\big((\alpha^2+\alpha\,\sigma+2)\,I_{3/2}(\alpha)-\alpha^2\,\sigma\,I_{1/2}(\alpha)\big)\,H_2\big]\,\vartheta_2(\zeta)\\&\quad+[6\,B_2-24\,C_2-2\,\alpha\,\sigma\,E_2-2\,(3+\alpha\,\sigma)\,F_2\\&\quad-(4+\alpha\,\sigma)\,K_{3/2}(\alpha)\,G_2-(4+\alpha\,\sigma)\,I_{3/2}(\alpha)\,H_2\big]\\&\quad\times\gamma_m\,\vartheta_m(\zeta)\,\vartheta_2(\zeta)\\&\quad+\sum_{n=3}^{\infty}[-n\,(n-1)\,A_n-n\,(n-1)\,B_n\\&\quad-(n+1)\,(n+2)\,C_n-(n-2)\,(n-3)\,D_n\\&\quad+n\,((n-1)-\alpha\,\sigma)\,E_n+(n-1)\,(n+\alpha\,\sigma)\,F_n\\&\quad+\big(\big((n-1)\,(n+\alpha\,\sigma)+\alpha^2\big)\,K_{n-1/2}(\alpha)\\&\quad+\alpha^2\,\sigma\,K_{n-3/2}(\alpha)\big)\,G_n+\big(\big((n-1)\,(n+\alpha\,\sigma)+\alpha^2\big)\\&\quad\times I_{n-1/2}(\alpha)-\alpha^2\,\sigma\,I_{n-3/2}(\alpha)\big)\,H_n\big]\,\vartheta_n(\zeta)=0\end{aligned}\tag{A.3}$$

$$\begin{aligned}&\left[-10\,C_2-D_2-\alpha^2\,E_2+\frac{\alpha^2}{2}\,F_2\right]P_1(\zeta)\\&\quad+\big[-10\,C_2+2\,D_2-\alpha^2\,E_2-\alpha^2\,F_2\big]\,\gamma_m\,\vartheta_m(\zeta)\,P_1(\zeta)\\&\quad+\sum_{n=3}^{\infty}\left[-\frac{(4\,n+2)}{n-1}\,C_n+\frac{(6-4n)}{n}\,D_n-\frac{\alpha^2}{(n-1)}\,E_n\right.\\&\quad\left.+\frac{\alpha^2}{n}\,F_n\right]P_{n-1}(\zeta)=0\end{aligned}\tag{A.4}$$

$$\begin{aligned}&\big[\eta^2\,E_2+\eta^{-1}\,F_2+\sqrt{\eta}\,K_{3/2}(\alpha\,\eta)\,G_2+\sqrt{\eta}\,I_{3/2}(\alpha\,\eta)\,H_2\big]\\&\quad\times\vartheta_2(\zeta)+\big[2\,\eta^2\,E_2-\eta^{-1}\,F_2\big]\,\beta_m\,\vartheta_m(\zeta)\,\vartheta_2(\zeta)\\&\quad+\sum_{n=3}^{\infty}\big[\eta^n\,E_n+\eta^{-n+1}\,F_n+\sqrt{\eta}\,K_{n-1/2}(\alpha\,\eta)\,G_n\\&\quad+\sqrt{\eta}\,I_{n-1/2}(\alpha\,\eta)\,H_n\big]\,\vartheta_n(\zeta)=0\end{aligned}\tag{A.5}$$

$$\begin{aligned}&\big[2\,\eta\,E_2-\eta^{-2}\,F_2-\eta^{-1/2}\,\big(K_{3/2}(\alpha\,\eta)+\alpha\,\eta\,K_{1/2}(\alpha\,\eta)\big)\,G_2\\&\quad-\eta^{-1/2}\,\big(I_{3/2}(\alpha\,\eta)-\alpha\,\eta\,I_{1/2}(\alpha\,\eta)\big)\,H_2\big]\,\vartheta_2(\zeta)\\&\quad+\big[2\,\eta\,E_2+2\,\eta^{-2}\,F_2+\eta^{-1/2}\,(K_{3/2}(\alpha\,\eta)\,G_2\\&\quad+I_{3/2}(\alpha\,\eta)\,H_2)\big]\,\beta_m\,\vartheta_m(\zeta)\,\vartheta_2(\zeta)+\sum_{n=3}^{\infty}\big[n\,\eta^{n-1}\,E_n\\&\quad-(n-1)\,\eta^{-n}\,F_n-\eta^{-1/2}\,\big((n-1)\,K_{n-1/2}(\alpha\,\eta)\\&\quad+\alpha\,\eta\,K_{n-3/2}(\alpha\,\eta)\big)\,G_n-\eta^{-1/2}\,\big((n-1)\,I_{n-1/2}(\alpha\,\eta)\\&\quad-\alpha\,\eta\,I_{n-3/2}(\alpha\,\eta)\big)\,H_n\big]\,\vartheta_n(\zeta)=0\end{aligned}\tag{A.6}$$

$$\lambda^{-4}\left[\lambda^2 A_2+\lambda^5 B_2+C_2+\lambda^3 D_2-\lambda^2\right]\vartheta_2(\zeta)+\sum_{n=3}^{\infty}\lambda^{-n-2}\left[\lambda^2 A_n+\lambda^{2n+1}B_n+C_n+\lambda^{2n-1}D_n\right]\times\vartheta_n(\zeta)=0 \quad (A.7)$$

$$\lambda^{-3}\left[2\lambda^2 A_2-\lambda^5 B_2+4C_2+\lambda^3 D_2-2\lambda^2\right]\vartheta_2(\zeta)+\sum_{n=3}^{\infty}\lambda^{-n-1}\left[n\lambda^2 A_n-(n-1)\lambda^{2n+1}B_n+(n+2)C_n-(n-3)\lambda^{2n-1}D_n\right]\vartheta_n(\zeta)=0. \quad (A.8)$$

Equating the leading coefficients in (A.1)–(A.8) to zero and solving the resulting system of equations, we get

$$A_2=(S_6 z_1+S_7 z_2+S_8 z_3+S_9 z_4+S_{10} z_5+S_{11} z_6)/\Delta, \quad (A.9)$$

$$B_2=(S_{12} z_1+S_{13} z_2+S_{14} z_3+S_{15} z_4+S_{16} z_5+S_{17} z_6)/\Delta, \quad (A.10)$$

$$C_2=(S_{18} z_1+S_{19} z_2+S_{20} z_3+S_{21} z_4+S_{22} z_5+S_{23} z_6)/\Delta, \quad (A.11)$$

$$D_2=(S_{24} z_1+S_{25}(\eta z_2+z_3)+S_{26} z_4+S_{27} z_5+S_{28} z_6)/\Delta, \quad (A.12)$$

$$E_2=\left(-6\eta^{3/2}S_{28} z_3+S_{29} z_4+S_{30} z_5\right)/\Delta, \quad (A.13)$$

$$F_2=-\eta\,(\eta S_{30}(3z_1+\alpha\eta z_5)+12\alpha\eta^{1/2}(S_{28}+90\lambda^5)z_3+S_{29}\eta(\alpha\eta z_4+3z_6))/(\alpha\Delta), \quad (A.14)$$

$$G_2=\left(3\sqrt{\eta}(S_{30}I_{1/2}(\alpha)+S_{29}I_{3/2}(\alpha))+S_{31}I_{1/2}(\alpha\eta)-18\eta^2 S_{28}I_{3/2}(\alpha\eta)\right)/(\alpha\Delta), \quad (A.15)$$

$$H_2=\left(3\sqrt{\eta}(S_{30}K_{1/2}(\alpha)-S_{29}K_{3/2}(\alpha))+S_{31}K_{1/2}(\alpha\eta)+18\eta^2 S_{28}K_{3/2}(\alpha\eta)\right)/(\alpha\Delta), \quad (A.16)$$

where

$\Delta=S_1 z_1+S_2(\eta z_2+z_3)+S_3 z_4+S_4 z_5+S_5 z_6,$

$z_1=I_{1/2}(\alpha)K_{3/2}(\alpha\eta)+I_{3/2}(\alpha\eta)K_{1/2}(\alpha),$

$z_2=I_{1/2}(\alpha)K_{3/2}(\alpha)+I_{3/2}(\alpha)K_{1/2}(\alpha),$

$z_3=I_{3/2}(\alpha\eta)K_{1/2}(\alpha\eta)+I_{1/2}(\alpha\eta)K_{3/2}(\alpha\eta),$

$z_4=I_{3/2}(\alpha)K_{1/2}(\alpha\eta)+I_{1/2}(\alpha\eta)K_{3/2}(\alpha),$

$z_5=I_{1/2}(\alpha)K_{1/2}(\alpha\eta)-I_{1/2}(\alpha\eta)K_{1/2}(\alpha),$

$z_6=I_{3/2}(\alpha)K_{3/2}(\alpha\eta)-I_{3/2}(\alpha\eta)K_{3/2}(\alpha),$

$S_1=-3\eta^2\left(180\lambda^5+4\alpha^2\lambda_1+\alpha^3\sigma\lambda_2+4\alpha\sigma\lambda_3\right),$

$S_2=6\sqrt{\eta}\left(90\lambda^5-\alpha^2\lambda_4+2\alpha\sigma\lambda_3\right),$

$S_3=-540\lambda^5+\alpha^3(\alpha+\sigma)(\eta^3+2)\lambda_2+12\alpha^2(15\eta^3\lambda^5(\lambda-1)+\lambda_5)-12\alpha\sigma\lambda_3,$

$S_4=-\alpha\left(180(\eta^3-1)\lambda^5+\alpha^2(\eta^3+2)(4\lambda_6+\alpha\sigma\lambda_2)+4\alpha\sigma(\eta^3-1)\lambda_3\right),$

$S_5=3\alpha\eta^2\left(180(\lambda-1)\lambda^5+\alpha(\alpha+\sigma)\lambda_2\right),$

$S_6=3\eta^2\left(-180\lambda^5+2\alpha^2\lambda_7+\alpha^3\sigma\lambda_8+4\alpha\sigma\lambda_9\right),$

$S_7=6\sqrt{\eta}\left(90\lambda^5+\alpha^2\lambda_{10}-2\alpha\sigma\lambda_9\right),$

$S_8=6\eta^{3/2}\left(90\lambda^5+\alpha^2\lambda_{11}-2\alpha\sigma\lambda_9\right),$

$S_9=-540\lambda^5-\alpha^3(\alpha+\sigma)(\eta^3+2)\lambda_8-12\alpha^2(15\eta^3\lambda^5+\lambda_{12})+12\alpha\sigma\lambda_9,$

$S_{10}=\alpha\left(-180(\eta^3-1)\lambda^5+2\alpha^2(\eta^3+2)\lambda_7+\alpha^3\sigma(\eta^3+2)\lambda_8+4\alpha\sigma(\eta^3-1)\lambda_9\right),$

$S_{11}=-3\alpha\eta^2\left(180\lambda^5+\alpha(\alpha+\sigma)\lambda_8\right),$

$S_{12}=6\alpha\eta^2(\alpha\lambda_{15}+\alpha^2\sigma\lambda_{18}+4\sigma\lambda_{16}),$

$S_{13}=12\alpha\sqrt{\eta}\lambda_{16}(\alpha-2\sigma),$

$S_{14}=12\alpha\eta^{3/2}(\alpha\lambda_{15}-2\sigma\lambda_{16}),$

$S_{15}=2\alpha\left(-\alpha^3(\alpha+\sigma)(\eta^3+2)\lambda_{18}-3\alpha(2\lambda_{15}+15\eta^3\lambda^3)+12\alpha\lambda_{16}\right),$

$S_{16}=2\alpha^2\left(\alpha(\eta^3+2)(\lambda_{15}+\alpha\sigma\lambda_{18})+4\sigma(\eta^3-1)\lambda_{16}\right),$

$S_{17}=-6\alpha\eta^2(45\lambda^3+\alpha(\alpha+\sigma)\lambda_{18}),$

$S_{18}=-9\alpha\eta^2\lambda^3(2\lambda^2(\alpha-2\sigma)+\alpha^2\sigma\lambda_{19}),$

$S_{19}=18\alpha\sqrt{\eta}\lambda^5(\alpha-2\sigma),$

$S_{20}=-36\alpha\eta^{3/2}\lambda^5(\alpha+\sigma),$

$S_{21}=3\alpha\lambda^3(12\lambda^2+\alpha^2(\eta^3+2)\lambda_{19})(\alpha+\sigma),$

$S_{22}=-3\alpha^2\lambda^3\left(\alpha(\eta^3+2)(2\lambda^2+\alpha\sigma\lambda_{19})-4(\eta^3-1)\lambda^2\sigma\right),$

$S_{23}=9\alpha^2\eta^2\lambda^3(\alpha+\sigma)\lambda_{19},$

$S_{24}=-18\alpha\eta^2\left(5(\alpha+4\sigma)\lambda^5+\alpha^2\sigma\lambda_{17}\right),$

$S_{25}=6\alpha\left(15\alpha(3\eta^3+2)\lambda^5+\alpha^2(\eta^3+2)(\alpha+\sigma)\lambda_{17}-60\lambda^5\sigma\right),$

$S_{26}=-6\alpha^2\left(\alpha(\eta^3+2)(5\lambda^5+\alpha\sigma\lambda_{17})+20(\eta^3-1)\lambda^5\sigma\right),$

$S_{27}=18\alpha\eta^2\left(45\lambda^5+\alpha(\alpha+\sigma)\lambda_{17}\right),$

$S_{28}=-90\lambda^5+\alpha^2\lambda_{13}-2\alpha\sigma\lambda_{14},$

$S_{29}=12\left(45\lambda^5+\alpha(\alpha+\sigma)\lambda_{14}\right),$

$S_{30}=-12\alpha\left(\alpha\sigma\lambda_{16}-3\lambda^5(5+2\alpha\sigma)\right),$

$S_{31}=6\alpha\left(-90\eta^3\lambda^5+(\eta^3+2)(\alpha^2\lambda_{13}-2\alpha\sigma\lambda_{14})\right),$

$\lambda_1=5\lambda^6-9\lambda^5+5\lambda^3-1,$

$\lambda_2=4\lambda^6-9\lambda^5+10\lambda^3-9\lambda+4,$

$\lambda_3=20\lambda^6-9\lambda^5-10\lambda^3-1,$

$\lambda_4=20\lambda^6-27\lambda^5+5\lambda^3+2,$

$\lambda_5=10\lambda^6-21\lambda^5+10\lambda^3+1,$

$\lambda_6=5\lambda^6-9\lambda^5+5\lambda^3-1,$

$\lambda_7=18\lambda^5-5\lambda^3+2, \qquad \lambda_8=9\lambda^5-5\lambda^3-4,$

$\lambda_9=9\lambda^5+5\lambda^3+1,$

$\lambda_{10}=27\lambda^5-10\lambda^3-2, \qquad \lambda_{11}=27\lambda^5+5\lambda^3-2,$

$\lambda_{12}=21\lambda^5-5\lambda^3-1,$

$\lambda_{13}=3\lambda^5-5\lambda^3+2, \qquad \lambda_{14}=6\lambda^5-5\lambda^3-1,$

$\lambda_{15}=5\lambda^3-2, \qquad \lambda_{16}=5\lambda^3+1,$

$\lambda_{17}=\lambda^5-1, \qquad \lambda_{18}=\lambda^3-1, \qquad \lambda_{19}=\lambda^2-1,$

$\lambda_{20}=4\lambda^2-1.$

To obtain the remaining arbitrary constants A_n, B_n, C_n, D_n, E_n, F_n, G_n, H_n, we require the following identities (see [1, p. 142])

$$\vartheta_m(\zeta)\vartheta_2(\zeta)=b_{m-2}\vartheta_{m-2}(\zeta)+b_m\vartheta_m(\zeta)+b_{m+2}\vartheta_{m+2}(\zeta) \quad (A.17)$$

$$\vartheta_m(\zeta)P_1(\zeta)=a_{m-2}P_{m-3}(\zeta)+a_m P_{m-1}(\zeta)+a_{m+2}P_{m+1}(\zeta) \quad (A.18)$$

where

$$b_{m-2}=-\frac{(m-2)(m-3)}{2(2m-1)(2m-3)},$$

$$b_m=\frac{m(m-1)}{(2m+1)(2m-3)},$$

$$b_{m+2} = -\frac{(m+1)\,(m+2)}{2\,(2m-1)\,(2m+1)},$$
$$a_{m-2} = \frac{(m-2)}{(2m-1)\,(2m-3)},$$
$$a_m = \frac{1}{(2m+1)\,(2m-3)},$$
$$a_{m+2} = -\frac{(m+1)}{(2m-1)\,(2m+1)}.$$

Using these in (A.1)–(A.8), we get

$$A_n = B_n = C_n = D_n = E_n = F_n = G_n = H_n = 0 \quad \text{for } n \neq m-2, m, m+2 \tag{A.19}$$

and when $n = m-2, m, m+2$, we have the following system

$$A_n + B_n + C_n + D_n - E_n - F_n - K_{n-1/2}(\alpha)\,G_n - I_{n-1/2}(\alpha)\,H_n = \xi_1\,b_n\,\gamma_m \tag{A.20}$$

$$n\,A_n - (n-1)\,B_n + (n+2)\,C_n - (n-3)\,D_n - n\,E_n + (n-1)\,F_n + \big((n-1)\,K_{n-1/2}(\alpha) + \alpha\,K_{n-3/2}(\alpha)\big)\,G_n + \big((n-1)\,I_{n-1/2}(\alpha) - \alpha\,I_{n-3/2}(\alpha)\big)\,H_n = \xi_2\,b_n\,\gamma_m \tag{A.21}$$

$$-n\,(n-1)\,A_n - n\,(n-1)\,B_n - (n+1)\,(n+2)\,C_n - (n-2)\,(n-3)\,D_n + n\,((n-1) - \alpha\,\sigma)\,E_n + (n-1)\,(n+\alpha\,\sigma)\,F_n + \big(\big((n-1)\,(n+\alpha\,\sigma) + \alpha^2\big) \times K_{n-1/2}(\alpha) + \alpha^2\,\sigma\,K_{n-3/2}(\alpha)\big)\,G_n + \big(\big((n-1)\,(n+\alpha\,\sigma) + \alpha^2\big)\,I_{n-1/2}(\alpha) - \alpha^2\,\sigma\,I_{n-3/2}(\alpha)\big)\,H_n = \xi_3\,b_n\,\gamma_m \tag{A.22}$$

$$-\frac{(4\,n+2)}{n-1}\,C_n + \frac{(6-4n)}{n}\,D_n - \frac{\alpha^2}{(n-1)}\,E_n + \frac{\alpha^2}{n}\,F_n = \xi_4\,a_n\,\gamma_m \tag{A.23}$$

$$\eta^n\,E_n + \eta^{-n+1}\,F_n + \sqrt{\eta}\,K_{n-1/2}(\alpha\,\eta)\,G_n + \sqrt{\eta}\,I_{n-1/2}(\alpha\,\eta)\,H_n = \xi_5\,b_n\,\beta_m \tag{A.24}$$

$$n\,\eta^{n-1}\,E_n - (n-1)\,\eta^{-n}\,F_n - \eta^{-1/2} \times \big((n-1)\,K_{n-1/2}(\alpha\,\eta) + \alpha\,\eta\,K_{n-3/2}(\alpha\,\eta)\big)\,G_n - \eta^{-1/2}\,\big((n-1)\,I_{n-1/2}(\alpha\,\eta) - \alpha\,\eta\,I_{n-3/2}(\alpha\,\eta)\big)\,H_n = \xi_6\,b_n\,\beta_m \tag{A.25}$$

$$\lambda^2\,A_n + \lambda^{2\,n+1}\,B_n + C_n + \lambda^{2\,n-1}\,D_n = 0 \tag{A.26}$$

$$n\,\lambda^2\,A_n - (n-1)\,\lambda^{2\,n+1}\,B_n + (n+2)\,C_n - (n-3)\,\lambda^{2\,n-1}\,D_n = 0 \tag{A.27}$$

where

$$\xi_1 = (2\,A_2 - B_2 + 4\,C_2 + D_2 - 2\,E_2 + F_2),$$
$$\xi_2 = (2\,A_2 + 2\,B_2 + 12\,C_2 - 2\,E_2 - 2\,F_2 - K_{3/2}(\alpha)\,G_2 - I_{3/2}(\alpha)\,H_2),$$
$$\xi_3 = (6\,B_2 - 24\,C_2 - 2\,\alpha\,\sigma\,E_2 - 2\,(3+\alpha\,\sigma)\,F_2 - (4+\alpha\,\sigma)\,K_{3/2}(\alpha)\,G_2 - (4+\alpha\,\sigma)\,I_{3/2}(\alpha)\,H_2),$$
$$\xi_4 = (-10\,C_2 + 2\,D_2 - \alpha^2\,E_2 - \alpha^2\,F_2),$$
$$\xi_5 = (2\,\eta^2\,E_2 - \eta^{-1}\,F_2),$$
$$\xi_6 = (2\,\eta\,E_2 + 2\,\eta^{-2}\,F_2 + \eta^{-1/2}\,(K_{3/2}(\alpha\,\eta)\,G_2 + I_{3/2}(\alpha\,\eta)\,H_2)).$$

The above system of equations is solved using MATHEMATICA version 5.2 and the expressions for A_n, B_n, C_n, D_n, E_n, F_n, G_n and H_n are obtained and contain the coefficients γ_m and β_m. As the expressions are cumbersome, they are not presented here.

The expressions for the constants $\mathscr{D}_2'$ and $\mathscr{D}_2''$ appearing in Eq. (6.2) are defined as

$$\mathscr{D}_2' = 2\,\big(\eta^{3/2}\,(2\,\xi_1\,\phi_1 + \alpha\,\xi_2\,\phi_2 + \xi_3\,\phi_3 - \xi_4\,\phi_4)\,\gamma_2 + \alpha\,(-2\,\xi_5\,\phi_5 + \eta\,\xi_6\,\phi_6)\,\beta_2\big)/(\eta^{3/2}\,\Delta) \tag{A.28}$$

$$\mathscr{D}_2'' = \big(-\eta^{3/2}\,(2\,\xi_1\,\phi_1 + \alpha\,\xi_2\,\phi_2 + \xi_3\,\phi_3 + 4\,\xi_4\,\phi_4)\,\gamma_4 + \alpha\,(2\,\xi_5\,\phi_5 - \eta\,\xi_6\,\phi_6)\,\beta_4\big)/(2\,\eta^{3/2}\,\Delta) \tag{A.29}$$

where

$$\phi_1 = 3\,\eta^2\,(-60\,\lambda^5 + \alpha^2\,\lambda_7 + \alpha^3\,\sigma\,\lambda_{14})\,z_1 + 90\,(\alpha^2+2)\,\lambda^5\,\sqrt{\eta}\,z_2 + 6\,\eta^{3/2}\,(30\,\lambda^5 + \alpha^2\,\lambda_{14})\,z_3 - (180\,\lambda^5 + \alpha^2\,(\eta^3+2)\,(15\,\lambda^3\,\lambda_{20} + \alpha\,(\alpha+\sigma)\,\lambda_{14}))\,z_4 + \alpha\,(-60\,(\eta^3-1)\,\lambda^5 + \alpha^2\,(\eta^3+2)\,(\lambda_7 + \alpha\,\sigma\,\lambda_{14}))\,z_5 - 3\,\alpha\,\eta^2\,(15\,\lambda^3\,\lambda_{20} + \alpha\,(\alpha+\sigma)\,\lambda_{14})\,z_6,$$

$$\phi_2 = 3\,\sigma\,\eta^2\,(60\,\lambda^5 - \alpha^2\,\lambda_{13})\,z_1 - 180\,\sqrt{\eta}\,\sigma\,\lambda^5\,z_2 + 90\,\eta^{3/2}\,\lambda^5\,(\alpha - 2\,\sigma)\,z_3 - (90\,\alpha\,\eta^3\,\lambda^5 - \alpha^2\,(\alpha+\sigma)\,(\eta^3+2)\,\lambda_{13} + 180\,\sigma\,\lambda^5)\,z_4 - \alpha\,\sigma\,(60\,(\eta^3-1)\,\lambda^5 - \alpha^2\,(\eta^3+2)\,\lambda_{13})\,z_5 - 3\,\eta^2\,(90\,\lambda^5 - \alpha\,(\alpha+\sigma)\,\lambda_{13})\,z_6,$$

$$\phi_3 = 3\,\eta^2\,(60\,\lambda^5 - \alpha^2\,\lambda_{13})\,z_1 - 180\,\sqrt{\eta}\,\lambda^5\,z_2 + 6\,\eta^{3/2}\,(30\,\lambda^5 + \alpha^2\,\lambda_{14})\,z_3 - 15\,\lambda^3\,(12\,\lambda^2 + \alpha^2\,(\eta^3+2)\,\lambda_{19})\,z_4 - \alpha\,(60\,(\eta^3-1)\,\lambda^5 - \alpha^2\,(\eta^3+2)\,\lambda_{13})\,z_5 - 45\,\alpha\,\eta^2\,\lambda^3\,\lambda_{19}\,z_6,$$

$$\phi_4 = 2\,(\alpha\,\sigma\,\lambda_{16} - 3\,\lambda^5\,(5+2\,\alpha\,\sigma))(3\,\eta^2\,z_1 - 3\,\eta^{3/2}\,z_3 + \alpha\,(\eta^3-1)\,z_5) - 3\,\sqrt{\eta}\,(30\,\lambda^5 - \alpha^2\,\lambda_{13} + 2\,\alpha\,\sigma\,\lambda_{14})\,z_2 - 3\,(30\,\lambda^5 + \alpha^2\,(2\,\lambda_{17} - 5\,\eta^3\,\lambda^3\,\lambda_{19}) - 2\,\alpha\,\sigma\,\lambda_{14})\,z_4 + 45\,\alpha\,\eta^2\,\lambda^3\,\lambda_{19}\,z_6,$$

$$\phi_5 = 3\,\alpha\,\eta^{3/2}\,(\alpha\,\sigma\,\lambda_{16} - 3\,\lambda^5\,(5+2\,\alpha\,\sigma))(z_1 + \alpha\,\eta\,z_5) + 3\,\eta^{3/2}\,(45\,\lambda^5 + \alpha\,(\alpha+\sigma)\,\lambda_{14})(z_6 + \alpha\,\eta\,z_4) - \alpha\,(90\,\eta^3\,\lambda^5 - \alpha^2\,(\eta^3-1)\,\lambda_{13} + 2\,\alpha\,\sigma\,(\eta^3-1)\,\lambda_{14})\,z_2,$$

$$\phi_6 = -6\,\alpha\,\eta^{3/2}\,(\alpha\,\sigma\,\lambda_{16} - 3\,\lambda^5\,(5+2\,\alpha\,\sigma))\,z_1 - \alpha\,(90\,\eta^3\,\lambda^5 - \alpha\,(\eta^3+2)\,(\alpha\,\lambda_{13} - 2\,\sigma\,\lambda_{14}))\,z_2 - 6\,\eta^{3/2}\,(45\,\lambda^5 + \alpha\,(\alpha+\sigma)\,\lambda_{14})\,z_6.$$

The expressions for the constants Δ_1, Δ_2 and Δ_3 appearing in Eq. (6.3) are defined as

$$\Delta_1 = -3\,\alpha\,\big(3\,\eta^2\,\omega_1 + \alpha\,(2+\eta^3)\,\omega_2\big)/(2\,\Delta), \tag{A.30}$$

$$\Delta_2 = \big(\eta^{3/2}\,(\alpha\,(\xi_7\,\phi_7 + \xi_8\,\phi_8 + \xi_9\,\phi_9) + \xi_{10}\,\phi_{10})\,\gamma_2 + \alpha\,(\xi_{11}\,\phi_{11} + \xi_{12}\,\phi_{12})\,\beta_2\big)/(\eta^{3/2}\,\Delta), \tag{A.31}$$

$$\Delta_3 = \big(-\eta^{3/2}\,(\alpha\,(\xi_7\,\phi_7 + \xi_8\,\phi_8 + \xi_9\,\phi_9) - 4\,\xi_{10}\,\phi_{10})\,\gamma_4 + \alpha\,(\xi_{11}\,\phi_{11} + \xi_{12}\,\phi_{12})\,\beta_2\big)/(4\,\eta^{3/2}\,\Delta) \tag{A.32}$$

where

$$\omega_1 = -z_1\,\alpha\,\sigma + z_6\,(\alpha+\sigma),$$
$$\omega_2 = -z_5\,\alpha\,\sigma + z_4\,(\alpha+\sigma),$$
$$\Delta = 3\,\eta^2\,\big(\alpha + \sigma\,(1-\alpha^2)\big)\,z_1 + \big(-3\,\sqrt{\eta}\,(z_2 + \eta\,z_3) + (3+\alpha^2\,(\eta^3+2))\,z_4 + 3\,\alpha\,\eta^2\,z_6\big) \times (\alpha+\sigma) + \big(\alpha^2\,(\eta^3+2)\,(1-\alpha\,\sigma) + \alpha\,\sigma\,(\eta^3-1)\big)\,z_5,$$
$$\xi_7 = 3\,\big(\big(3\,\eta^2\,(-\alpha\,z_1 + z_6) + \alpha\,(\eta^3+2)\,(z_4 - \alpha\,z_5)\big)\,(\alpha+\sigma) + 3\,\alpha^2\,\sqrt{\eta}\,z_2\big)/(\alpha\,\Delta),$$
$$\phi_7 = \alpha\,(\eta^3+2)\,(\omega_2 + 2\,z_5) + 3\,\eta^2\,(\omega_1 + 2\,z_1) - 6\,\eta^{3/2}\,z_3,$$

$$\xi_8 = \left(3\,\left(3\,\alpha^3\,\eta^2\,z_1 + 3\,\alpha\,\sqrt{\eta}\,z_2 + \alpha^4\,(\eta^3+2)\,z_5\right)\sigma - 3\,\alpha\,(1+\alpha^2)\,(\eta^3+2)\,(\alpha+\sigma)\,z_4 - 9\,\eta^2\,(1+\alpha^2)\,(\alpha+\sigma)\,z_6\right)/(\alpha\,\Delta),$$

$$\phi_8 = 3\,\eta^2\,\omega_1 + \alpha\,(\eta^3+2)\,\omega_2,$$

$$\xi_9 = 3\,\left(3\,\alpha\,\eta^2\,(2\,\sigma + \alpha\,(2+\sigma(\alpha+2\,\sigma)))\,z_1 - 3\,\alpha^2\,\sqrt{\eta}\,(2+\sigma^2)\,z_2 - 6\,\alpha^2\,\eta^{3/2}\,\sigma\,(\alpha+\sigma)\,z_3 - \alpha\,(\alpha+\sigma)\,\left((2+\alpha^2)\,(\eta^3+2) + \alpha\,\sigma\,(\eta^3-4)\right)\,z_4 + \alpha^2\,\left((2\,\alpha + (2+\alpha^2)\,\sigma)\,(\eta^3+2) + 2\,\alpha\,(\eta^3-1)\,\sigma^2\right)\,z_5 - 3\,\eta^2\,(\alpha+\sigma)\,(2+\alpha(\alpha+\sigma))\,z_6\right)/(\alpha\,\Delta),$$

$$\phi_9 = 3\,\eta^2\,(z_1 - \eta^{-1/2}\,z_3) + \alpha\,(\eta^3+2)\,z_5,$$

$$\xi_{10} = 9\,\alpha^2\,(\omega_2 - \eta^{3/2}\,(\alpha+\sigma)z_3)/\Delta,$$

$$\phi_{10} = -3\,\eta^2\,\sigma\,(z_1 - \eta^{-1/2}\,z_3) + 3\,(\alpha+\sigma)\,(\sqrt{\eta}\,z_2 - z_4) - \alpha\,\sigma\,(\eta^3-1)\,z_5,$$

$$\xi_{11} = -3\left(3\,\eta\,(\omega_1 + \alpha\,\eta\,\omega_2) - 2\,\alpha\,\sqrt{\eta}\,(\eta^3-1)\,(\alpha+\sigma)\,z_3\right)/(\alpha\,\Delta),$$

$$\phi_{11} = 3\,\eta^{3/2}\,(\omega_1 + \alpha\,\eta\,\omega_2) - 2\,\alpha\,(\eta^3-1)(\alpha+\sigma)z_2,$$

$$\xi_{12} = 3\,\left(3\,\sqrt{\eta}\,\omega_1 + \alpha\,(\eta^3+2)\,(\alpha+\sigma)\,z_3\right)/(\alpha\,\sqrt{\eta}\,\Delta),$$

$$\phi_{12} = 3\,\eta^{5/2}\,\omega_1 + \alpha\,\eta\,(\eta^3+2)\,(\alpha+\sigma)\,z_2.$$

References

[1] J. Happel, H. Brenner, Low Reynolds Number Hydrodynamics, Prentice-Hall, Englewood Cliffs, NJ, 1965.
[2] S. Kim, S.J. Karrila, Microhydrodynamics: Principles and Selected Applications, ButterworthHeinemann, Boston, MA, USA, 1991.
[3] E. Cunningham, On the velocity of steady fall of spherical particles through fluid medium, Proc. R. Soc. Lond. Ser. A 83 (1910) 357–365.
[4] W.E. Williams, On the motion of a sphere in a viscous fluid, Philos. Mag. 29 (1915) 526–550.
[5] W.L. Haberman, R.M. Sayre, Wall effects for rigid and fluid spheres in slow motion with a moving liquid, David Taylor model, Basin Report No. 1143, Washington, DC, 1958.
[6] H. Ramkissoon, K. Rahaman, Wall effects on a spherical particle, Int. J. Eng. Sci. 41 (2003) 283–290.
[7] H.C. Brinkman, A calculation of viscous force exerted by a flowing fluid on dense swarm of particles, Appl. Sci. Res. A 1 (1957) 27–34.
[8] H.J. Keh, J. Chou, Creeping motion of a composite sphere in a concentric spherical cavity, Chem. Eng. Sci. 59 (2004) 407–415.
[9] H.J. Keh, Y.S. Lu, Creeping motions of a porous spherical shell in a concentric spherical cavity, J. Fluids Struct. 20 (2005) 735–747.
[10] D. Srinivacharya, Motion of a porous sphere in a spherical container, C. R. Mec. 333 (2005) 612–616.
[11] D. Srinivasacharya, Creeping flow past a porous approximate sphere, Z. Angew. Math. Mech. 83 (2003) 499–504.
[12] Satya Deo, Bali Ram Gupta, Stokes flow past a swarm of porous approximately spheroidal particles with Kuwabara boundary condition, Acta Mech. 203 (2009) 241–254.
[13] E.I. Saad, Translation and rotation of a porous spheroid in a spheroidal container, Can. J. Phys. 88 (2010) 689–700.
[14] J.A. Ochoa-Tapia, S. Whitaker, Momentum transfer at the boundary between a porous medium and a homogeneous fluid I, theoretical development, Int. J. Heat Mass Transfer 38 (1995) 2635–2646.
[15] J.A. Ochoa-Tapia, S. Whitaker, Momentum transfer at the boundary between a porous medium and a homogeneous fluid II, comparison with experiment, Int. J. Heat Mass Transfer 38 (1995) 2647–2655.
[16] A.V. Kuznetsov, Analytical investigation of the fluid flow in the interface region between a porous media and a clear fluid in channels partially filled with porous medium, Appl. Sci. Res. 56 (1996) 53–67.
[17] A.V. Kuznetsov, Analytical investigation of Couette flow in a composite channel partially filled with a porous media and partially with a clear fluid, Int. J. Heat Mass Transfer 41 (1998) 2556–2560.
[18] Anindita Bhattacharyya, G.P. Raja Sekhar, Viscous flow past a porous sphere with an impermeable core: effect of stress jump condition, Chem. Eng. Sci. 59 (2004) 4481–4492.
[19] Anindita Bhattacharyya, G.P. Raja Sekhar, Stokes flow inside a porous spherical shell: stress jump boundary condition, Z. Angew. Math. Phys. 56 (2005) 475–496.
[20] A.C. Srivastava, N. Srivastava, Flow of a viscous fluid at small Reynolds number past a porous sphere with a solid core, Acta Mech. 186 (2006) 161–172.
[21] P.K. Yadav, A. Tiwari, S. Deo, S. Vasin, A. Filippov, Hydrodynamic permeability of membranes built up by spherical particles covered by porous shells: effect of stress jump condition, Acta Mech. 215 (2010) 193–209.
[22] B.S. Bhatt, Nirmal C. Sacheti, Flow past a porous spherical shell using Brinkman model, J. Phys. D: Appl. Phys. 27 (1) (1994) 37–41.
[23] G. Neale, N. Epstein, W. Nader, Creeping flow relative to permeable spheres, Chem. Eng. Sci. 28 (1973) 1865–1874.